Bulgarian Chemical Communications, Volume 49, Special Issue F, (pp. 107- 113) 2017

Preparation and characterization of palladium containing nickel-iron-cobalt perovskite catalysts for complete oxidation of propane

S. G. Stanchovska*, R. K. Stoyanova, E. N. Zhecheva, A. I. Naydenov

Institute of General and Inorganic Chemistry, Bulgarian Academy of Sciences, Acad. G. Bonchev Str., Bldg. 11, Sofia 1113, Bulgaria

Submitted on July 15, 2016; Revised on October 28, 2016

Palladium containing nickel-iron-cobalt perovskite catalysts $La(Co_{0.8}Ni_{0.1}Fe_{0.1})_{1-x}Pd_xO_3$ with x=0.05 and 0.15 were synthesized at 600 ºC from citrate precursors obtained by freeze-drying. Structural and morphological characterization was carried out by XRD, BET surface measurements, TEM and XPS. The reduction properties of catalysts were examined by TPR with H_2 combined with *ex-situ* XRD measurements. The results obtained indicate formation of cobalt-based perovskite phases in which Pd ions are incorporated into the crystal structure. For the sample with the higher Pd content, traces of PdO and/or $La_2Pd_2O_5$ also appear. The oxide compositions are studied as catalysts for complete oxidation of propane as model substance of saturated hydrocarbons. The reaction parameters as light-off temperatures (for achievement of 50 % conversion, T_{50}), pre-exponential factors and the apparent activation energies were determined, internal diffusion effect being taken into account within the applied reactor model. The observed increase in the reaction rate constant when palladium is incorporated in into the perovskite structure is accordance with the concentration and forms of the palladium, exposed on the catalytic surface.

Key words: palladium, cobalt perovskites, propane, complete oxidation

INTRODUCTION

The catalytic combustion of volatile organic compounds (VOCs) is considered as one of the best methods for waste gases purification. Noble metals and transition metal oxides are intensively studied as catalysts for VOCs neutralization. The "classical" exhaust catalysts contain noble metals (Pd, Pt, Rh) for pollutant treatment. The high price of the noble metals and limited abundance, as well as their sintering ability and sensitivity to catalytic poisons, are the driving force for the development of new catalysts for VOCs neutralization. Perovskite-type oxides containing transition metals are considered to be a promising catalyst for pollution abatement because of their low cost, high activity and thermal stability, which makes them potential alternatives to noble metals. In 1972 Voorhove was the first who reported the high catalytic activity of perovskite oxides for heterogeneous oxidation [1]. These studies stimulated a lot of research that was related to exhaust control catalysts (see, for example refs. [2-4]. Perovskites are mixed oxides with general formula ABO_3, where A is usually a lanthanide ion and B is a transition metal ion. The B-site cation is surrounded octahedrally by oxygen, and the A site cation is located in the cavity made by these octahedra. Both A and B ions can be partially substituted, leading to a wide variety of mixed oxides. For complete oxidation reactions, cation B is responsible for the catalytic activity [4], while cation A, especially when partially substituted by a cation of different oxidation state, governs the stabilization of unusual oxidation states for B, leading to different catalytic performance [4-6]. It has been reported that the highest catalytic activity belongs with lanthanum as metal A and Co, Mn, Fe and Ni as metal B [2,7,8]. For oxidation of CO and hydrocarbons, $LaCoO_3$ is demonstrated to be one of the most active perovskites [9]. In the last decade the interest in the perovskite catalysts revived, due to the elaboration of the so-called "intelligent" three-way catalysts based on Pd-containing perovskite oxides [10, 11]. It was established that these catalysts display self-regenerative function under operating conditions through the interaction of Pd (or other platinum group metals) with the perovskite lattice. In response to the periodic reducing and oxidizing reaction conditions in stoichiometric engines fuelled by natural gas, Pd segregates and re-dissolve into ABO_3 lattice, thus preventing extensive particle sintering under prolonged operation at high temperature [10, 12, 13].

Generally, the catalytic activity of the "intelligent" catalysts is governed by the chemical state and redox behavior of Pd, which, on its turn, depends on the composition of the perovskite phase as well as on the feed stream composition and operating conditions. The preparation method is of crucial importance for the activity of these catalysts [14-17].

In this study we present data on the synthesis of a Pd-containing Co-based perovskite oxide and the

* To whom all correspondence should be sent: E-mail: stanchovska@svr.igic.bas.bg

impact of Pd additives on the catalytic oxidation of propane as model substance for saturated hydrocarbons. In the cobalt perovskite studied, Ni and Fe were partially substituted for Co, since, according to ref. [18], these compositions display improved catalytic activity as compared to pure $LaCoO_3$. In order to ensure homogeneous distribution of Co, Ni, Fe and Pd, the samples were prepared using the citrate precursor method.

EXPERIMENTAL

Homogeneous La-Co-Ni-Fe-Pd citrate precursors for the target perovskite compositions $La(Co_{0.8}Ni_{0.1}Fe_{0.1})_{1-x}Pd_xO_3$, x=0, 0.05 and 0.15, were obtained by the freeze-drying method. La-Co-Ni-Fe and La-Co-Ni-Fe-Pd citrates were prepared by adding $La(NO_3)_2.6H_2O$, $CoCO_3$, $NiCO_3$, $Fe(NO_3)_2.xH_2O$ and $Pd(NO_3).xH_2O$ 5M to a 0.1M aqueous solution of citric acid (CA). After stirring at 60 °C, a clear solution was obtained. After concentration to 0.5 M La, the solution was cooled to room temperature, then frozen instantly with liquid nitrogen and dried under vacuum at -20 °C in an Alpha-Christ freeze dryer. The thermal decomposition of the citrate precursors was achieved at 400 °C for 3h in air. The obtained solid residue was annealed at 600 °C for 3 h in air.

X-ray structural analysis was performed on a Bruker Advance 8 diffractometer with Cu Kα radiation. Step-scan recordings for structure refinement by the Rietveld method were carried out using 0.02° 2θ steps of 5 s duration.

The TEM investigations were performed on a TEM JEOL 2100 instrument at accelerating voltage of 200 kV. The specimens were prepared by grinding and dispersing them in ethanol by ultrasonic treatment for 6 min. The suspensions were dripped on standard holey carbon/Cu grids. The analysis was carried out by the Digital Micrograph software.

The XPS measurements were carried out in the UHV chamber of the electron spectrometer ESCALAB MkII (VG Scientific) using a AlKα excitation source. The spectra calibration was performed by using the C 1s line of adventitious carbon, centred at binding energy (BE) of 285.0 eV.

The specific surface area of the catalysts was determined by low temperature adsorption of nitrogen according to the BET method using Nova 1200 (Quantachrome) apparatus. Temperature programmed reduction (TPR) experiments were carried out in the measurement cell of a differential scanning calorimeter (DSC), model DSC-111 (SETARAM), directly connected to a gas chromatograph (GC), in the 300–973 K range at a 10 K/min heating rate in a flow of $Ar:H_2$ = 9:1, the total flow rate being 20 ml/min. A cooling trap between DSC and GC removes the water obtained during the reduction. To obtain the ex situ XRD patterns of the partially reduced oxides, the reduction process was interrupted at selected temperatures and then the samples were cooled down to room temperature in an $Ar:H_2$ flow followed by Ar treatment for 10 min.

The catalytic activity tests were carried out in a continuous-flow type reactor. The following testing conditions were applied: catalyst bed volume of 0.5 cm^3, irregular shaped particles having an average diameter of 0.65 ± 0.15 mm, reactor diameter of 7.0 mm, quartz-glass ($D_{reactor}/D_{particles} \geq 10$). The gas hourly space velocity (GHSV) was fixed to 60 000 h^{-1}. The inlet concentration of propane was 0.1 vol. %, while the oxygen supply was kept at 20.9 vol.%. The gas mixture was balanced to 100 % with nitrogen (4.0). The gas analysis was performed using an on-line gas-analyzers of $CO/CO_2/O_2$ (Maihak) and THC-FID (total hydrocarbon content with a flame ionization detector, Horiba). For compensation of the adiabatic effect of the reaction, the catalyst bed temperature was maintained almost constant. The pressure drop of the catalytic bed was measured to be less than 2 kPa, and it was not taken into account. The axial dispersion effect was neglected as the catalyst bed is corresponding to a chain of more than 10 ideal-mixing cells along the reactor axis. Therefore the geometrical characteristics and the flow conditions of the catalytic reactor justify the conclusion that the reactor is close to the case of isothermal plug flow reactor (PFR) except for the effect of radial velocity profile inside the catalyst bed.

RESULTS AND DISSCUSIONS

Figure 1 displays the XRD diffraction patterns of $La(Co_{0.8}Ni_{0.1}Fe_{0.1})O_3$ and $La(Co_{0.8}Ni_{0.1}Fe_{0.1})_{1-x}Pd_xO_3$, x=0.05 and 0.15, obtained at 600 °C. The XRD peaks correspond to a rhombohedrally distorted perovskite phase (space group R-3c). No additional reflections are visible for $La(Co_{0.8}Ni_{0.1}Fe_{0.1})O_3$ and $La(Co_{0.8}Ni_{0.1}Fe_{0.1})_{1-x}Pd_xO_3$ with x=0.05. For $La(Co_{0.8}Ni_{0.1}Fe_{0.1})_{1-x}Pd_xO_3$ with x=0.15, additional low intensity peaks are observed which correspond to traces of impurity PdO and/or $La_2Pd_2O_5$ phases (inset of Fig. 1c).

The unit cell parameters of the perovskite phase for the three samples are listed in Table 1. The substitution of Pd for transition metal ions leads to a lattice expansion, which is in accordance with the

higher ionic radius of palladium ions (0.615 for Co^{3+} (low spin 0.545 Å), Ni^{3+} (low spin 0.56 Å, high spin 0.60 Å) and Fe^{3+} (0.645 Å).

The XRD results indicate the formation of perovskite phases in which Pd ions are incorporated into the crystal structure. This underlines an effectiveness of the citrate-precursor method for the preparation of perovskite oxides.

Table 1. Unit cell parameters and specific surface area of $La(Co_{0.8}Ni_{0.1}Fe_{0.1})_{1-x}Pd_xO_3$.

	a, Å	c, Å	V, Å^3	S, m^2/g
x=0	5.4482 (7)	13.1763 (22)	338.71 (8)	13
x=0.05	5.4479 (8)	13.1827 (23)	338.84 (9)	14
x=0.15	5.4576 (9)	13.2048 (31)	340.61 (11)	15

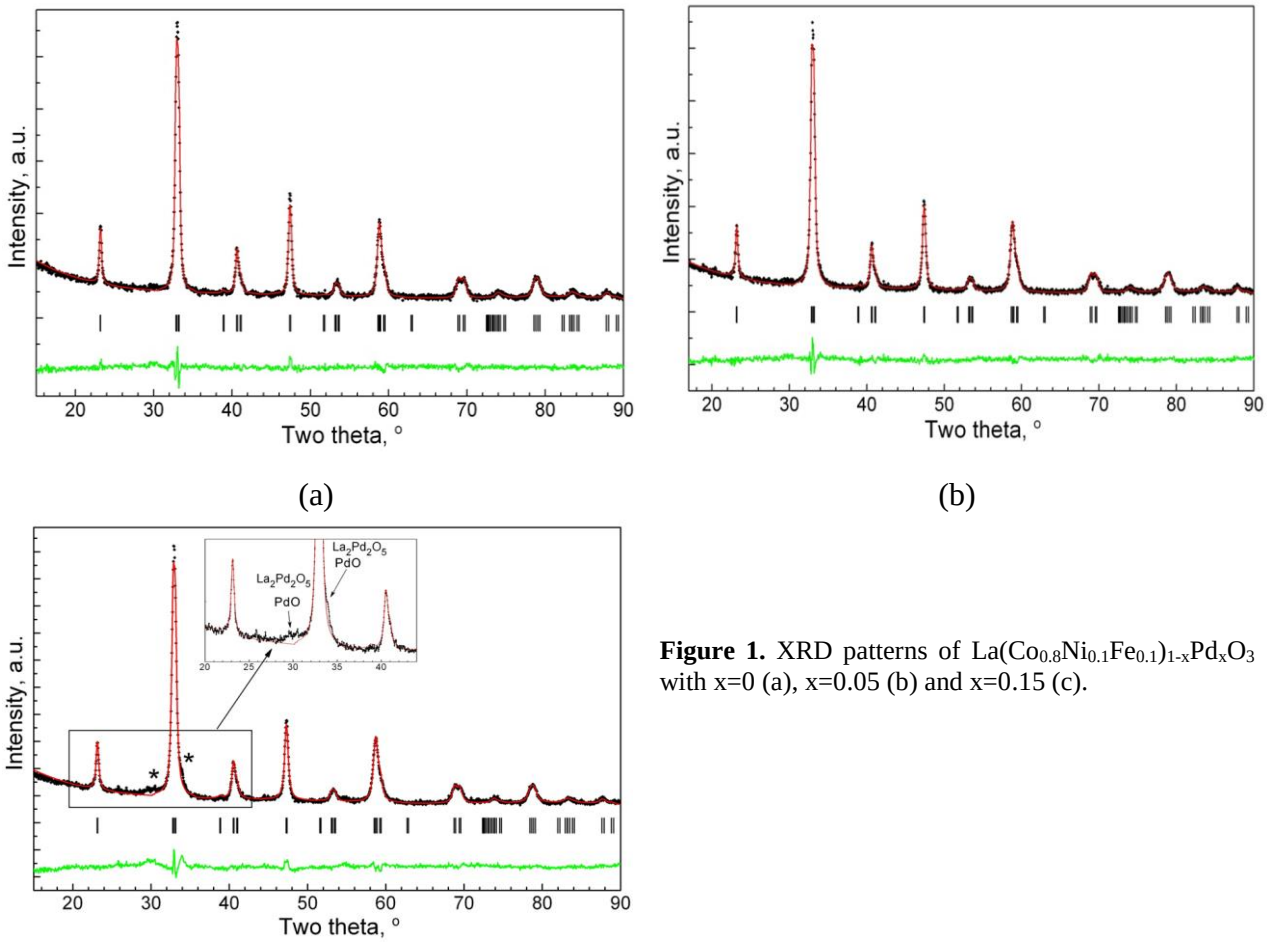

Figure 1. XRD patterns of $La(Co_{0.8}Ni_{0.1}Fe_{0.1})_{1-x}Pd_xO_3$ with x=0 (a), x=0.05 (b) and x=0.15 (c).

Palladium additives poorly affect the morphology of the perovskite phase. The specific surface areas have close values (13-15 m^2/g) and the particle sizes are in the nanometer range (30-50 nm, Figs. 2a and 2b). Figures 2a and 2b show the electron diffraction images of $La(Co_{0.8}Ni_{0.1}Fe_{0.1})_{1-x}Pd_xO_3$. It can be seen that both materials were polycrystalline with a rhombohedral perovskite as a main phase.

The oxidation states of Pd on the surface of the powder catalysts were analyzed by means of XPS. Figure 3 shows the Pd 3d3/2 and 3d5/2 core level spectra of $La(Co_{0.8}Ni_{0.1}Fe_{0.1})_{1-x}Pd_xO_3$. For $La(Co_{0.8}Ni_{0.1}Fe_{0.1})_{0.95}Pd_{0.05}O_3$ the Pd 3d5/2 peak is located at 338.1 eV and appears symmetrical (Fig. 3a). For the sample with the higher Pd content x=0.15 the experimental spectrum of Pd 3d5/2 is asymmetrical and can be deconvoluted into two peaks centered at 338.1 and 337.2 eV, respectively (Fig. 3b). The XPS spectra of Pd in palladium-containing perovskite catalysts in their oxidized and reduced form are presented in several papers [19-21]. The unusual high Pd 3d5/2 peak observed for these catalysts at about 337.7-338.2 eV was ascribed to Pd^{3+} or Pd^{4+} species inserted in the B-site of the perovskite structure, whereas the peak

with the lower energy at 336.1-336.6 corresponds to Pd^{2+} in PdO [19-21].

This means that for the $La(Co_{0.8}Ni_{0.1}Fe_{0.1})_{0.95}Pd_{0.05}O_3$ sample Pd is mostly incorporated into the perovskite structure, whereas for $La(Co_{0.8}Ni_{0.1}Fe_{0.1})_{0.85}Pd_{0.15}O_3$ the palladium ions are distributed between the perovskite phase and a Pd-rich phase (PdO or $La_2Pd_2O_5$) , the ratio between these two Pd species being of about 2:1. The Pd concentration in the surface layer of the two samples is close to that in the bulk: 3.6 and 4.6 at. % Pd in the surface versus 1.7 and 5 at. % for the bulk composition.

The amount and the forms of Pd in $La(Co_{0.8}Ni_{0.1}Fe_{0.1})_{1-x}Pd_xO_3$ is related with their thermal reduction properties. Figure 4 compares the TPR curves with H_2 of pure $La(Co_{0.8}Ni_{0.1}Fe_{0.1})O_3$ and the Pd containing samples. The TPR profiles of $La(Co_{0.8}Ni_{0.1}Fe_{0.1})O_3$ shows two successive

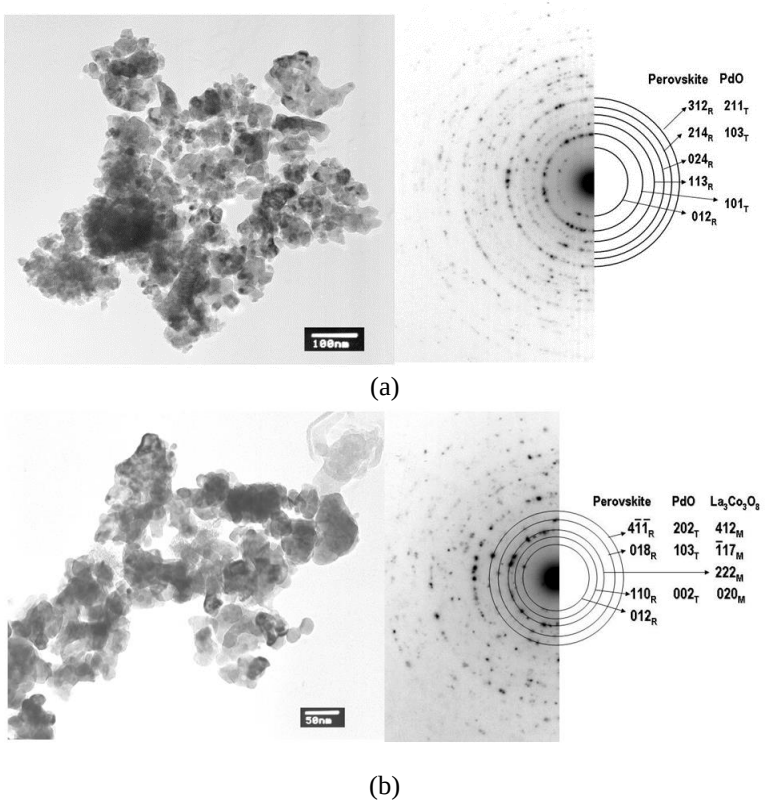

Figure 2. Bright field micrographs and polycrystalline electron diffractions of $La(Co_{0.8}Ni_{0.1}Fe_{0.1})_{0.95}Pd_{0.05}O_3$ (a) and $La(Co_{0.8}Ni_{0.1}Fe_{0.1})_{0.85}Pd_{0.15}O_3$ (b).

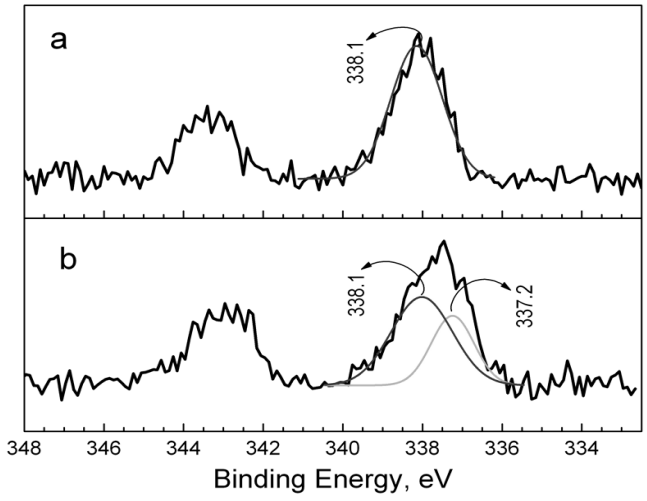

Figure 3. XPS spectra in the Pd 3d3/2 and Pd 3d5/2 regions for La $(Co_{0.8}Ni_{0.1}Fe_{0.1})_{0.95}Pd_{0.05}O_3$ (a) and La $(Co_{0.8}Ni_{0.1}Fe_{0.1})_{0.85}Pd_{0.15}O_3$ (b).

reduction peaks, the first one with T_{max}=420 °C and the other with T_{max}=570 °C. It is well documented that the reduction of $LaCoO_3$ is a two-staged process including a reduction of $LaCoO_3$ to La_2O_3 and Co^0 via the formation of intermediate Brownmillerite-type phases containing Co^{2+} ions [22-25]. The presence of Pd in the catalysts shifts the reduction of the perovskite phase to lower temperatures [21, 26-29]. For $La(Co_{0.8}Ni_{0.1}Fe_{0.1})_{1-x}Pd_xO_3$ samples Pd affects only the first reduction stage: for the sample with x=0.05 the first reduction stage is shifted to significantly lower temperatures and the peak is split into three components with T_{max}=86, 155 and 209 °C, respectively. For the sample with x=0.15 the reduction temperature is lowered remarkably, thus reaching values of T_{max} = 66 °C and 110 °C, respectively (Fig. 4). It is interesting to note that for both samples the second

stage of the reduction process is not affected by the presence of Pd in the catalysts. This means that the perovskite-derived Brownmillerite phases do not contain Pd.

In the literature, the first low-temperature peak with a low-intensity appearing in TPR curves has been explained by the reduction of Pd oxide species into Pd metal whereas the other peaks have been assigned to the reduction of Co^{3+} to Co^0 via Co^{2+} [30]. It is suggested that Pd facilitates the reduction of cobalt due to spillover of the dissociated hydrogen atoms which were formed on the palladium particles [30].

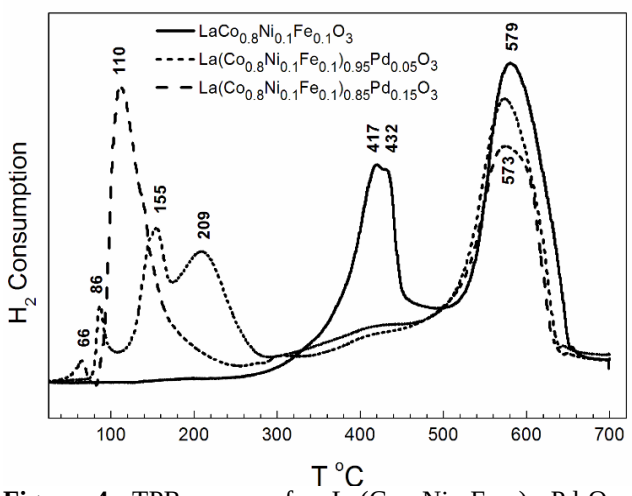

Figure 4. TPR curves for $La(Co_{0.8}Ni_{0.1}Fe_{0.1})_{1-x}Pd_xO_3$ perovskites.

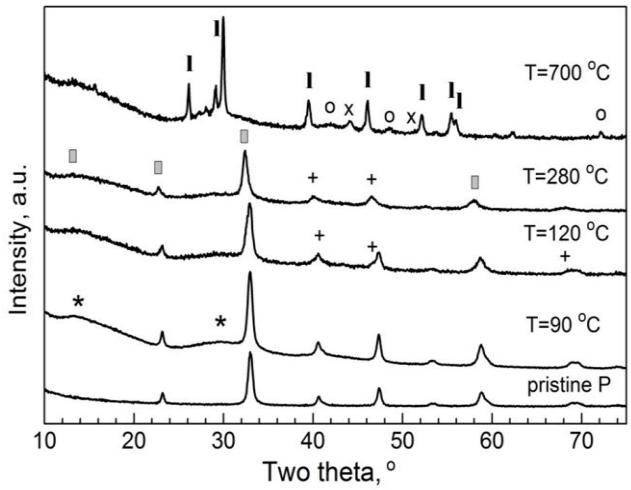

Figure 5. *ex-situ* XRD patterns of partially reduced $LaPd_{0.05}M_{0.95}O_3$. The symbols correspond to: * - $La_2Pd_2O_5$ or La_2PdO_4; + - Pd; ▮- $La_2Co_2O_5$, **I** – La_2O_3; o – CoPd; x – Co/Ni.

To rationalize the observed difference in reducibility of $La(Co_{0.8}Ni_{0.1}Fe_{0.1})_{1-x}Pd_xO_3$, *ex-situ* XRD measurements of partially and completely reduced samples were undertaken. The reduced compositions were obtained after interrupting the reduction process at selected temperatures. The reduction of $La(Co_{0.8}Ni_{0.1}Fe_{0.1})_{0.95}Pd_{0.05}O_3$ starts below 100 °C with the separation of La-Pd oxide phases of the type $La_2Co_2O_5$ or La_2PdO_4 from the Co-perovskite matrix (Fig. 5). Reduction up to 120 °C leads to the formation of metallic Pd and oxygen-deficient perovskite phases, $LaMO_{3-\delta}$. At 280 °C, the reduction of Co^{3+} to Co^{2+} is completed and Co-brownmillerite is formed. The end products of the reduction of $La(Co_{0.8}Ni_{0.1}Fe_{0.1})_{0.95}Pd_{0.05}O_3$ are CoPd, Co/Ni metals and La_2O_3. Hence, in the case of Pd substituted perovskites, the reduction of the Pd species to metallic Pd is preceded by their separation from the perovskite phase, $La_2Pd_2O_5$ or La_2PdO_4 oxides containing Pd^{2+} being formed.

In order to examine the applicability of the synthesized materials as combustion catalysts, the reaction of complete oxidation of propane was investigated. The results from catalytic experiments are presented in Figure 6. The data from the conversion – temperature dependencies were used for fitting the kinetics parameters by using of one – dimensional pseudo-homogeneous model of plug-flow isothermal reactor [31,32].

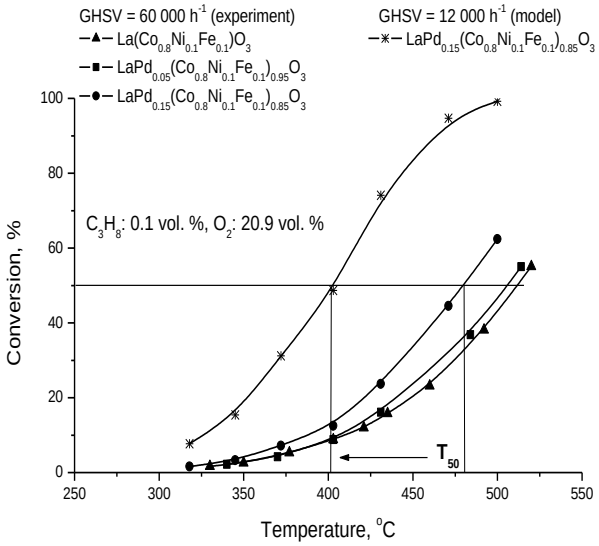

Figure 6. Dependencies of the conversion on the reaction temperature during complete oxidation of hydrocarbons on $La(Co_{0.8}Ni_{0.1}Fe_{0.1})O_3$ and $La(Co_{0.8}Ni_{0.1}Fe_{0.1})_{1-x}Pd_xO_3$, x=0.05 and 0.15.

For the calculations of the pre-exponential factors (k_o) and the apparent activation energies (E_{app}), data for conversions below 20-25 % were utilized. At such reaction conditions the calculated values for the average effectiveness factors (accounting for the irregular shaped catalyst particles) were within the limits 0.87–0.99 and therefore the effect of the internal diffusion effect had to be implemented in the reactor model by

applying of an iterative approach. The calculated reaction parameters are presented in Table 2.

The calculated values for the apparent activation energies are very close (within the limits of the experimental error), thus leading to the assumption for similarity of the reaction mechanism. Further, the model calculations show that at gas-hourly space velocity of 12 000 h^{-1} the expected T_{50} can be lowered with about 80 °C, which can be considered as a promising basis for development of catalyst for cleaning of waste gases containing saturated hydrocarbons (conversion of 99 % can be reached at 500 °C (GHSV = 12 000 h^{-1}).

Table 2. Reaction parameters for the complete oxidation of hydrocarbons on $La(Co_{0.8}Ni_{0.1}Fe_{0.1})O_3$ and $La(Co_{0.8}Ni_{0.1}Fe_{0.1})_{1-x}Pd_xO_3$, x = 0, 0.05 and 0.15.

Catalyst:	X = 0	X = 0.05	X =0.15
T_{50}, [°C]	511	505	479
k_o, [s^{-1}]	1.67 x 10^7	2.88 x 10^7	1.09 x 10^8
$E_{app,}$ [kJ/mol]	87	89	94

As stated above, the XRD results indicate a formation of cobalt-based perovskite phases in which Pd ions are incorporated into the crystal structure. The quantitative analysis of the reaction rate parameters show that the incorporation of palladium in the basic composition with x=0.05 leads to an increase in the reaction rate constant with about 10 %, while the effect of x=0.15 is in the range of 70 %. When similar comparative analysis is applied to the Pd - containing samples only, the average increase of the reaction rate constants (Pd from x=0.05 to x=0.15) is 54 %, i.e. much less than the expected tentatively three times higher activity if the effect of the added palladium was proportional to its content. However, this result is in better accordance with the XPS – data for the concentration and forms of the palladium, exposed on the catalytic surface – the difference in the rate constants in this case is in the range of 30 % (higher being for x =0.15 sample). It should be pointed out that in our case XRD – results revealed that within the x=0.05 sample Pd is mostly incorporated into the perovskite structure, whereas for x=0.15 the palladium ions are distributed between the perovskite phase and a Pd-rich phase (PdO or $La_2Pd_2O_5$), at ratio between these two Pd species being of about 2:1. As reported by Eyssler at all [20], the highest catalytic activity for similar samples was measured for catalysts where palladium was predominantly dispersed as supported PdO particles thus stating that Pd incorporation in the perovskite-type lattice may not be favorable for methane oxidation. However, the main goal is the finding of stable palladium – based combustion catalyst and the incorporation of palladium within the perovskite-type lattice is a perspective approach to prevent sintering phenomena [20].

CONCLUSIONS

Using citrate precursors, monophase perovskite oxide $La(Co_{0.8}Ni_{0.1}Fe_{0.1})_{0.95}Pd_{0.05}O_3$ can be prepared at 600 °C, in which the Pd ions are incorporated into the perovskite structure. For higher Pd content, traces of PdO and/or $La_2Pd_2O_5$ also appear .The amount and the forms of Pd in $La(Co_{0.8}Ni_{0.1}Fe_{0.1})_{1-x}Pd_xO_3$ catalysts affect their thermal reduction properties. Pd has a significant effect on the reduction temperature of Co^{3+} to Co^{2+}, intermediate cobalt Brownmillerite - type phases that do not contain Pd being formed.

The observed increase in the reaction rate constant when palladium is incorporated into the perovskite structure is accordance with the concentration and forms of the palladium, exposed on the catalytic surface. Despite that the incorporation of palladium within the perovskite-type lattice leads to some lowering of the catalytic activity when compared to Pd/PdO – based samples, the applied approach for synthesis of materials with prevented sintering properties and self-regenerative function can be considered as perspective in searching of stable palladium – based combustion catalyst.

REFERENCES

1. R.J.H. Voorhove, J.P. Remeika, P.E. Freeland, B.T. Mathias, *Science*, **177**, 353 (1972).
2. T. Siyama, *Catal. Rev. – Sci. Eng*., **34**, 281 (1992).
3. L. G. Tejuca, J. L. C. Fierro, Properties and Application of Perovskite-type Oxides, Marcel Dekker eds., New York, 1993.
4. W.B. Li, J. X. Wang, H. Gong, *Catal. Today*, **148**, 81 (2009).
5. M. S. Islam, M. Cherry, C. R. Catlow, *J. Solid State Chem*., **124**, 230 (1996).
6. R. Leanza, I. Rossetti, L. Fabbrini, C. Oliva, L. Forni, *Appl. Catal. B*, **28**, 55 (2000).
7. S. Cimino, L. Lisi, S. De Rossi, M. Faticanti, P. Porta, *Appl. Catal. B*, **83**, 214 (2008).

8 B. Kucharczyk, W. Tylus, *Catal. Today*, **90**, 121 (2004).
9. M. A. Pena, J. L. G. Fierro, *Chem. Rev*., **101**, 1981 (2001).
10 Y. Nishihata, J. Mizuki, T. Akao, H. Tanaka, M. Uenishi, M. Kimura, T. Okamoto, N. Hamada, *Nature*, **418**, 164 (2002).
11 H. Tanaka, M. Taniguchi, M. Uenishi, N. Najita, I. Tan, Y. Nishihata, J. Mizuki, K. Narita, M. Kimura, K. Kaneko, *Angewandte Chemie*, **45**, 5998 (2006).
12. J. P. Dacquin, M. Cabie, C. R. Henry, C. Cancelot, C. Dujardun, C. R. Raout, P. G. Granger, *J. Catal*., **270**, 299 (2010).
13. M. B. Katz, G. W. Graham, Y. Duan, H. Liu, C. Adamo, D. G. Schlom, X. Pan, *J. Amer. Chem. Soc.*, **133**, 18090 (2011).
14. E. Campagnoli, A. Tavares, L. Fabbrini, I. Rossetti, Yu.A.Dubitsky, A. Zaopo, L. Forni, *Appl. Catal. B*, **55**, 133 (2005).
15. M. M. Natile, E. Ugel, C. Maccoto, A. Glisenti, *Appl. Cat*al. *B*, **72,** 351 (2007).
16. A. E. Giannakas, A. K. Lavados, P. J. Pomonis, *Appl. Catal. B*, **49**, 147 (2004).
17. E. Tzimpilis, N. Moshoudis, M. Stoukides, P. Bekiaroglou, *Appl. Catal. B*, **84,** 607 (2008).
18. S. Stanchovska, E. Zhecheva, R. Stoyanova, A. Naydenov, unpublished results.
19. M. Uenishi, M. Taniguchi, H. Tanaka, M. Kimura, Y. Nishihata, J. Mizuki, T. Kobayashi, *Appl. Catal. B*, **57**, 267 (2005).
20. A. Eyssler, P. Mandaliev, A. Winkler, P. Hug, O. Safonova, R. Figi, A. Weidenkaff, D. Ferri, J. *Phys. Chem. C*, **114,** 4584 (2010).
21. A. Eyssler, A. Winkler, O. Safonova, M. Nachtegal, S. K. Matam, P. Hug, A. Eidenkaff, D. Ferri, *Chem. Mater*., **24**, 1865 (2012).
22. O. H. Hansteen, H. Fjellvag, B. C.Hauback, *J. Mater. Chem.*, **8**, 2081 (1998).
23. C. L. Charello, J. –D. Grunwald, D. Ferri, F. Krumeich, C. Oliva, L. Forni, A. Baiker, *J. Catal*., **252,** 127 (2005).
24. S. Ivanova, A. Senyshyn, E. Zhecheva, K. Tenchev, R. Stoyanova, H. Fuess, *J. Solid State Chem.*, **183,** 940 (2010).
25. S. Ivanova, A. Senyshyn, E. Zhecheva, K. Tenchev, V. Nikolov, R. Stoyanova, H. Fuess, *J. Alloys Compd*., **480**, 279 (2009).
26. J. P. Dacquin, C. Dujardin, P. J. Granger, *J. Catal.*, **253**, 37 (2008).
27. S. Sartipi, A. A. Khodadadi, Y. Mortazavi, *Appl. Catal. B*, **83**, 214 (2008).
28. J.–M. Giraudon, A. Elhachimi, F. Wyrwalski, S. Siffert, A. Aboukais, J. F. Lamonier, G. Leclercq, *Appl. Catal. B*, **75**, 157 (2007).
29. H. Ziaei-Azad, A. Khodadadi, P. Esmaeilnejad-Ahranjani, Y. Mortazavi, *Appl. Catal. B*, **102**, 62 (2011).
30. W. J. Chen, M. Okumura, Y. Matsumura, M. Haruta, *Appl. Catal. A*, **213**, 225 (2001).
31. F. Duprat, *Chem. Eng. Sci.*, **57**, 901 (2002).
32. P. Harriot, Chemical Reactor Design, Marcel Dekker, Inc. (2003).

СИНТЕЗ И ОХАРАКТЕРИЗИРАНЕ НА СЪДЪРЖАЩИ ПАЛАДИЙ НИКЕЛ-ЖЕЛЯЗО-КОБАЛТОВИ ПЕРОВСКИТОВИ КАТАЛИЗАТОРИ ЗА ПЪЛНО ОКИСЛЕНИЕ НА ПРОПАН

С. Г. Станчовска*, Р. К. Стоянова , Е. Н. Жечева, А. И. Найденов

Институт по обща и неорганична химия, Българска академия на науките, бул. Акад. Г. Бончев, бл. 11, София 1113, България

Постъпила на 15 юли, 2016 г. коригирана на 28 октомври, 2016 г.

(Резюме)

Паладий-съдържащи перовскитови катализатори със състав $La(Co_{0.8}Ni_{0.1}Fe_{0.1})_{1-x}Pd_xO_3$, x=0.05 и 0.15, са синтезирани при 600 °C от лиофилизирани цитратни прекурсори. XRD, измервания на специфичната повърхност по метода на BET, TEM и XPS са използвани за структурното и морфологично охарактеризиране на образците, а редукционните им свойства са изучени чрез TPR с H_2 в комбинация с *ex-situ* XRD имервания на междинните продукти. Показано е образуването на смесени кобалтови перовскити, в които Pd йони са включени в кристалната структура. При катализатора с по-високо съдържание на Pd се наблюдават и следи от PdO и / или $La_2Pd_2O_5$. Перовскитите са изследвани като катализатори за пълно окисление на пропан като моделно съединение на наситените въглеводороди. Определени са реакционните параметри като температурата за достигане на конверсия от 50 %, предекспоненциалния фактор и наблюдаемата активираща енергия, като в използвания модел на реактор е отчетено влиянието на вътрешната дифузия. Установено е, че вграждането на паладия в перовскитовата кристална структура води до повишаване стойността на скоростната константа на реакцията, като нарастването корелира с концентрацията и формите на паладия в приповърхностния слой на катализаторите.